GSA DATA REPOSITORY 2012238 Bacon et al.

Supplementary Material

Detailed ^{10}Be Extraction, Isotopic Measurement, and Data Reduction Methods

Soil and saprolite samples were sieved with a 2 mm screen, depth composited by mass, and pulverized with a shatterbox at Duke University prior to ^{10}Be extraction. Meteoric ^{10}Be was extracted from the pulverized samples in the University of Vermont's cosmogenic nuclide extraction laboratory. Samples were prepared in a batch of 16 following a modification of the flux fusion method presented by Stone (1998). We included two full process blanks with 14 unknowns and the sample from 1.5–2.0 m was run in replicate.

About 0.5 g of sample material was mixed with KHF and $NaSO_4$ along with ~300 ug of Be (SPEX brand carrier). The mixture was fused in a platinum crucible for several minutes until the melt was clear. After cooling, the crucible containing the solidified fusion cake was rapidly submerged into a Teflon beaker containing Milli-Q water (18.2 Mohm), heated, and allowed to leach overnight. Excess K was removed by $HClO_3$ precipitation and Be was precipitated as BeOH which was washed and dried. The hydroxide was burned to BeO, mixed with an equimolar amount of niobium metal powder, and loaded into stainless steel cathodes for isotopic analysis at the Center for Accelerator Mass Spectrometry, Lawrence Livermore National Laboratory.

Beryllium isotopic ratios were measured using multiple analyses of each target. Analyses of each target were repeated between 3 and 6 times until the precision (the greater of the internal and external uncertainties) of each unknown measurement (excepting the blanks) was < 1% (1σ; m = 0.6 ± 0.1%). Initial beam currents were very high for these samples, ranging from 21.9 to 31.1 μA with an average of 25.2 μA; this compares to an average beam current for standards run with these samples of 21.8 μA. Three secondary standards were run repeatedly to verify linearity of the AMS. Results were normalized to 07KNSTD3110 with a reported ^{10}Be/^{9}Be ratio of $2.85 \cdot 10^{-12}$ (Nishiizumi et al., 2007). Normalized isotopic ratios were corrected for isobaric interference from boron-10 (< 0.01%), and ranged from $5250 \cdot 10^{-15}$ to $11790 \cdot 10^{-15}$. We made a blank correction by subtracting the average long-term (n = 23, June 2008–Dec 2009) process blank for the UVM meteoric ^{10}Be extraction lab ($16.3 \pm 1.4 \cdot 10^{-15}$) from each measured sample ratio. The two blanks run with these samples (16.2 ± 0.7 and $19.5 \pm 0.8 \cdot 10^{-15}$) are consistent with this long-term average. We subtracted blank ratios from sample ratios because all samples contained similar amounts of carrier. Because these samples contained so much ^{10}Be and the average sample ratio was high (n = 14, m = $8300 \cdot 10^{-15}$), the resulting blank correction is inconsequential (< 0.4%). The replicate sample reproduced well giving ^{10}Be concentrations of 2.92 ± 0.02 (1σ) and $2.96 \pm 0.02 \cdot 10^{8}$ atoms g^{-1}, respectively.

Immobile Reference Element Selection

Since no element is completely immobile in soils we evaluated both zirconium (Zr) and titanium (Ti) for use as the immobile reference element in our mass balance analysis. We chose

Zr as the immobile element for three reasons. First, in the greater than 30 m of unweathered granite gneiss that we sampled, Zr concentrations are considerably less variable than that of Ti (Table DR2). This suggests that differences in Zr concentrations of individual soil samples are less likely to be a result of inherent parent material variability than Ti concentrations. Second, the elevated concentrations of Ti in illuvial horizons (0.3–1.5 m) relative to directly overlying horizons suggest translocation within the soil system. Conversely, Zr concentrations in the surficial horizons are larger than that of any other horizon; what should be expected of an immobile element as most other elements are removed from these elluvial horizons (Figure DR3). Lastly, in laboratory batch experiments, Zr has been observed to be less mobile than Ti in granite systems (Neaman et al., 2006).

Long-Term Surface Erosion (ε)

Although we lack measurements of ε from the interfluve that we sampled we constrained long-term surface erosion between $3.5 \cdot 10^{-5}$ cm yr^{-1} and $3.0 \cdot 10^{-4}$ cm yr^{-1}, and assume that the true ε is captured in this broad range. Measurements of *in-situ* ^{10}Be from an upland Ultisol in the Southern Piedmont show ε is $<3.0 \cdot 10^{-4}$ cm yr^{-1} (Lal et al., 1996). Basin scale analysis of *in-situ* ^{10}Be average erosion of diversely eroding features and suggest that as a landscape ε is between $3.0 \cdot 10^{-4}$ and $21.0 \cdot 10^{-4}$ cm yr^{-1} in the Southern Piedmont (Trodick, 2011). Considering that the interfluve surfaces we and Lal et al. (1996) sampled are certainly the most slowly eroding features of the landscape, $3.0 \cdot 10^{-4}$ cm yr^{-1} is a reasonable maximum bound of ε. Contemporary erosion from nearly level interfluves under "primeval" forest cover in the region proceeds much slower, and has been measured as low as $2 \cdot 10^{-3}$ tons acre^{-1} annually, or $3.5 \cdot 10^{-5}$ cm yr^{-1} if bulk density equals 1.25 g cm^{-3} (Smith and Stamey, 1965). This rate is an effective minimum bound of ε because such a low rate is thought to be untenable over geologic time (Portenga and Bierman, 2011).

Supplementary References Cited

Lal, D., Pavich, M., Gu, Z. Y., Jull, A. J. T., Caffee, M., Finkel, R., Southon, J., 1996, Recent erosional history of a soil profile based on cosmogenic ^{14}C and ^{10}Be: Geophysical Monograph Series, v. 95, p. 371-376, doi:10.1029/GM095p0371.

Neaman, A., Chorover, J., and Brantley, S. L., 2006, Effects of organic ligands on granite dissolution in batch experiments at pH6: American Journal of Science, v. 306, p. 451-473, doi:10.2475/06.2006.03.

Nishiizumi, K., Imamura, M., Caffee, M., Southon, J. R., R. Finkel, C., and McAninch, J., 2007, Absolute calibration of ^{10}Be standards: Nuclear Instruments and Methods in Physics Research Section B: Beam Interactions with Materials and Atoms, v. 258, p. 403-413, doi:10.1016/j.nimb.2007.01.297.

Portenga, E. W. and Bierman, P. R., 2011, Understanding Earth's eroding surface with ^{10}Be: GSA Today, v. 21, p. 4-10, doi:10.1130/G111A.1.

Smith, R. M. and Stamey, W. L., 1965, Determining the range of tolerable erosion: Soil Science, v. 100, p. 414-424.

TABLE DR1. VARIABILITY OF PHYSICAL AND CHEMICAL PROPERTIES BETWEEN THE THREE CONTINOUS CORES.

Hor	Depth (m)	ρ* g/cm^3	Clay (%)	Sand (%)	pH	C (%)	ECEC (cmol/kg)	EBS (%)	totZr	totCa	totAl (mg/g)	totFe	hheFe†	tot^{9}Be (ug/g)	hhe^{9}Be†	^{10}Be† (10^8atm/g)
A	0.00–0.07	0.17	0.2	0.3	0.10	0.10	0.2	3.4	0.02	0.01	0.58	0.46	-	0.07	-	-
AE	0.07–0.13	0.02	0.2	0.6	0.09	0.09	0.0	4.4	0.02	0.07	1.15	0.43	-	0.06	-	
E	0.13–0.32	0.06	0.8	1.2	0.11	0.02	0.1	2.1	0.04	0.01	2.31	0.54	-	0.01	-	-
Bt	0.32–0.6	0.06	2.6	2.0	0.03	0.03	0.0	2.9	0.01	0.04	10.97	3.59	-	0.27	-	-
Bt	0.6–1.0	-	3.4	2.2	0.05	0.01	0.5	4.4	0.02	0.01	3.46	2.08	-	0.04	-	-
Bt	1.0–1.5	-	3.8	3.6	0.05	0.01	0.9	3.1	0.02	0.01	5.77	3.74	-	0.08	-	-
BC	1.5–2.0	-	2.0	5.4	0.05	0.01	1.0	2.2	0.04	0.01	9.24	2.58	-	0.05	-	-
CB	2.0–2.5	-	2.0	3.4	0.06	0.01	1.1	1.3	0.01	0.01	6.35	1.42	-	0.07	-	-
CB	2.5–3.0	-	2.0	4.0	0.06	<0.01	0.5	0.9	0.02	0.00	6.35	0.84	-	0.04	-	-
C	3.0–3.5	-	1.2	3.2	0.02	<0.01	0.6	1.4	0.02	0.00	6.93	1.97	-	0.05	-	-
C	3.5–4.0	-	0.9	3.2	0.02	<0.01	0.9	2.5	0.01	0.01	4.04	2.52	-	0.08	-	-
C	4.0–4.5	-	1.3	2.5	0.01	0.01	1.9	2.6	0.02	0.01	4.04	2.33	-	0.02	-	-
C	4.5–5.0	-	0.9	2.4	0.03	0.01	0.7	1.3	0.03	0.01	4.04	1.66	-	0.08	-	-
C	5.0–5.5	-	0.9	1.5	0.03	<0.01	0.6	1.3	0.03	0.02	7.51	0.68	-	0.10	-	
C	5.5–6.1	-	0.6	1.5	0.01	<0.01	0.4	1.6	0.05	0.02	4.04	1.72	-	0.10	-	-

Note: Values reported here are standard errors between the 3 continuous cores. Values not reported below 6.1 m where n=1 core.
* ρ variability reported for our direct estimates, but not reported below 0.6 m where ρ estimates are derived elsewhere (see Table 1).
†Property estimated on composited samples, therefore variability not reported.

TABLE DR2. TOTAL ELEMENTAL CONCENTRATIONS OF UNWEATHERED GRANITIC GNEISS UNDERLYING THE SOUTHERN PIEDMONT ULTISOL.

Depth (m)	Zr (mg g^{-1})	Ca (mg g^{-1})	Fe (mg g^{-1})	^{9}Be (ug g^{-1})	Ti (ug g^{-1})
30.5–33.5	0.33	13.41	16.97	1.91	3.17
33.5–36.6	0.32	14.21	14.51	1.89	3.34
36.6–39.6	0.18	12.61	9.94	1.36	1.72
39.6–42.7	0.23	13.16	12.33	1.28	2.04
42.7–45.7	0.20	14.82	12.37	1.74	1.83
45.7–48.8	0.24	14.23	11.49	2.18	1.64
48.8–51.8	0.23	13.47	12.03	1.42	2.00
51.8–54.9	0.22	13.00	12.60	1.70	1.99
54.9–57.9	0.19	11.95	10.17	2.51	1.60
57.9–61.0	0.18	11.90	9.56	3.09	1.61
61.0–64.0	0.16	8.78	7.11	4.57	1.10
64.0–67.1	0.24	14.11	11.64	1.60	1.85
Mean	0.23	12.97	11.73	2.10	1.99
Standard Error	0.02	0.46	0.72	0.27	0.19
Coefficient of Variation (%)	23	12	21	44	32

Figure DR1. A: Location and parent material distribution of the Southern Piedmont (Richter and Markewitz, 2001). B: Topography of the sampling location with 10 m contour lines.

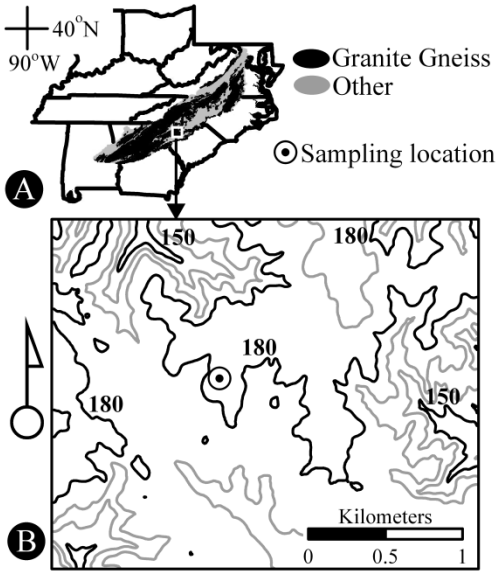

Figure DR2. Strong agreement between hhe iron extracted with 1 M $NH_2OH{\cdot}HCl$ in 1 M HCl (present study) and with dithionite citrate bicarbonate (Fimmen et al., 2008) from the same soil at two locations (approximately 500 m apart) on the same interfluve. Vertical lines represent the integrated sampling depth in each analysis.

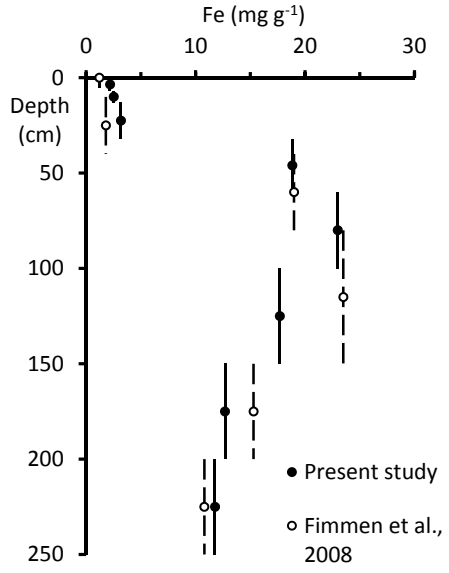

Figure DR3. Total elemental concentrations of zirconium (Zr) and Titanium (Ti) in the Southern Piedmont Ultisol.